Shape of free and constrained group-IV crystallites: Influence of surface energies

A. A. Stekolnikov and F. Bechstedt
Institut für Festkörpertheorie und -optik, Friedrich-Schiller-Universität, 07743 Jena, Germany
(Received 15 June 2004; revised manuscript received 18 May 2005; published 16 September 2005)

The equilibrium crystal shapes of the group-IV materials diamond, Si, and Ge are constructed based on surface energies obtained by means of *ab initio* calculations. The same method is applied to constrained crystallites with a pyramidal shape and a fixed orientation of the basal plane. Trends of shape are discussed versus the constraints and the orientation of facets using only energetical arguments.

DOI: 10.1103/PhysRevB.72.125326 PACS number(s): 61.46.+w, 68.35.Md, 68.43.Hn, 68.47.Fg

I. INTRODUCTION

Nanoscale fabrication has driven renewed interest in self-organization and self-assembly at surfaces. The central topic is the formation of self-assembled islands, or quantum dots, during epitaxial growth.[1–3] It is characterized by several distinct island shapes, unusual island size distributions, and certain island arrangements. There is an understanding of island nucleation[4] and subsequent coarsening (Ostwald ripening)[5] for the simple case where islands grow with a fixed shape. However, the island shape, the change in the shape of growing islands, and the precise nature of shape transitions have been the subject of intense discussions.[6] Theories of elastic relaxation at surfaces predict the formation and stabilization of periodic structures with defined sizes.[7] In such analyses, the island size is determined by balancing the elastic energy gain associated with the relaxation at the phase boundary against the energy cost of creating the boundary. However, it is difficult to establish the link between stress and morphology because key kinetic or thermodynamic parameters necessary for a quantitative interpretation are often unknown. Furthermore, the microscopic rearrangement of the atoms on the surfaces to minimize the local energies may play an important role.[8]

A prototypical example for the island formation is the Stranski-Krastanov (SK) growth mode[3,8,9] of Ge on Si(100) substrates. The growth of a strained wetting layer, as thick as 3–4 monolayers, is followed by the formation of three-dimensional islands. Eaglesham and Cerullo[10] have made the surprising discovery that in the initial stages of SK growth, the islands can be coherent, i.e., dislocation-free. Only later, as the islands grow in size, they become dislocated. The coherent islands can be up to ~150 nm in size and ~50 nm high. Before the appearance of micrometer-sized Ge crystallites an intermediate phase of metastable clusters has been also observed.[11] Scanning tunneling microscopy (STM) at low Ge coverage has shown that small islands (so-called hut clusters[11] or pyramids[12]) with rectangular or square base are formed by {501} facets. Larger islands with a higher aspect ratio, so-called domes,[13,14] appear at higher Ge coverages and display a multifaceted surface including {311} facets. The situation may be more complicated due to intermixing. Recently, it has been shown[15] that domes contain a Si-rich core covered by a Ge-rich shell.

The situation is less clear for Si crystallites. Micrometer-scale Si droplets have been formed on a Si(111) substrate by photolithography.[16] They have been used to determine the equilibrium shape of a small Si crystal. Well-characterized {111} and {311} facets exist on the surface. They are separated by rounded regions that display a tangential merging into the facets. Bermond *et al.*[16] found that the surface energy increases from {100} to {111} via a {311} plane and has local minima at the low-index surfaces {111}, {311}, {110}, and {100}. These results are in qualitative agreement with measurements[17] of nanometer-sized voids in a Si crystal that indicate the existence of the same facets. Pyramidal Si nanocrystals can be selectively grown on Si(100) windows in ultrathin SiO_2 films.[18–21] These Si pyramids possess four equivalent facets of the type {111}, {311} or even {911} and {1 3 11}. Using a microshadow mask technology or nonplanar prepatterned Si(100) substrates, the self-assembling MBE growth also leads to nanometer-scale features.[22] Depending on the growth parameters, pyramidlike tips or long wedges are formed. The sidewalls are free-standing {111} and {311} facets.

Small synthetic diamonds grown by high-pressure–high-temperature methods have major growth sectors of {100} and {111} type and some minor sectors of {110} and {311}.[23] The morphology of diamond particles grown at high temperature by means of chemical vapor deposition (CVD) is dominated by {100} and {111} facets (see Ref. 24 and references therein). In addition, facets of the type {110} and {311} appear between those with common orientation. However, it is difficult to conclude that {311} facets exist in a steady state. Using CVD, also diamond nanocrystallites can be grown partially epitaxially or perfectly heteroepitaxially on stepped Si substrates with [110] orientation.[25] An exact determination of the facet orientations of the crystallites with 2–6 nm size is hardly possible.

The actual three-dimensional shape of a free crystallite or a nanocrystal grown on a certain substrate depends on many thermodynamic and kinetic aspects or growth conditions. In this paper, we focus the attention on purely thermodynamic considerations. More precisely, we restrict the discussions of the shapes to pure energetic arguments. This approach may be sufficient for free crystallites but not for nanocrystallites (hetero)epitaxially grown on certain substrates. In this case, strain may play a dominant role for the crystallite shape.[1,26] Nevertheless, interesting trends can already be derived studying the energetics. Such a discussion requires the knowledge of the exact surface energies in dependence on the surface orientation and even the surface reconstruction. Unfortu-

TABLE I. Surface energies γ (in J/m^2) for diamond, Si, and Ge.[28–30] The first value represents the unrelaxed $\{hkl\}$ surface, while the second (lower) value corresponds to the reconstructed and relaxed geometry with the lowest energy. In the case of Si the results are compared with those of measurements[17] (the absolute scale is set using the value $\gamma(111)$ from fracture experiments,[33]) tight-binding calculations,[31] and molecular dynamics with empirical potentials.[32] A reconstruction is not taken into account. Only the measured $\gamma(111)$ value should be related to the 2×1 reconstruction.[33]

Crystal	{111}	{110}	{100}	{311}	Refs.
Diamond	8.12	7.48	9.72	8.34	
	4.06	5.93	5.71	5.11	28 and 29
Silicon	1.82	2.04	2.39	2.21	
	1.36	1.63	1.41	1.40	28–30
	1.23	1.43	1.36	1.38	17
	1.41	1.57	1.34	1.98	31
	1.41	1.72	1.49		32
Germanium	1.32	1.51	1.71	1.61	
	1.01	1.14	1.00	0.99	28–30

nately, a complete and well-accepted set of corresponding experimental data is not available. In general, the experimental determination of absolute surface energies remains a challenge.[27] However, in recent years results of accurate first-principles calculations have been published for absolute surface energies of diamond, silicon, and germanium. There are now values for {111}, {110}, {100}, and {311} planes with various reconstructions.[28–30] Consequently, we restrict the studies to group-IV materials. We begin with a discussion of the surface energies in Sec. II. The equilibrium crystal shapes are described in Sec. III, and pyramidal shapes of nanocrystals with fixed orientation and basal plane are discussed in Sec. IV. A summary and conclusions follow in Section V.

II. ABSOLUTE SURFACE ENERGIES

A. Computational method

The fact that crystal surfaces tend naturally to take particular orientations is probably the most familiar attribute of crystals. The tendency is driven by the surface tension γ, which is usually defined as the reversible work done in creating a unit area of a new surface.[3] An equivalent view is that γ is the surface excess density of Kramer's grand potential, which is minimized at constant temperature, volume, and chemical potentials. Consequently, it can be identified as the surface excess free energy per unit area or the surface energy for short, but imprecisely.[26] The calculation of such energies is easier for group-IV materials and small temperatures compared to the melting temperature.[26,28] Using a centrosymmetric slab with appropriate orientation $\{hkl\}$, the surface energy $\gamma=\gamma(hkl)$ follows as the half difference of the total energy of the slab with surfaces and the total energy of the corresponding bulk divided by the surface area. Converged *ab initio* calculations are performed using up to 24 atomic layers and a vacuum region corresponding to 36 atomic layers.[28]

B. Dependence on orientation and reconstruction

Resulting values[28–30] depending on the surface orientation and the surface reconstruction are summarized in Table I. If one imagines cutting a group-IV crystal at some plane, one may expect the energy required to be proportional to the number of bonds cut. In units of a_0^{-2} (a_0, bulk lattice constant) the dangling-bond density across a {111} surface plane is $4/\sqrt{3}$. This is smaller than the density of $2\sqrt{2}$ on a {110} surface, $12/\sqrt{11}$ on a {311} surface, and 4 on a {100} surface. With exception of diamond the trends in the energies of the unrelaxed and unreconstructed Si and Ge surfaces follow the dangling-bond densities. However, after inclusion of surface reconstruction the {111} surfaces of diamond possess the lowest energy, and therefore one may expect the natural cleavage plane or growth surface to be a {111} surface. There are eight such orientations, forming the eight faces of the natural octahedral crystal for the homopolar tetrahedral solids. The ordering of the other surface energies is more complicated to understand. With surface reconstruction, the {311} faces seem to be favored against the {110} planes (cf., e.g., in the case of diamond). This is in agreement with the dangling-bond densities if only the dangling bonds in the uppermost atomic layer of the {311} surface are counted. The high surface energies $\gamma(110)$ for silicon and germanium in Table I reflect the small energy gain of only about 0.5 eV/1×1 unit cell, even studying the long-range 16×2 reconstructions.[30] The final atomic structures of Si and Ge(110) surfaces are under discussion. The absolute surface energies of the reconstructed {111}, {311}, and {100} surfaces of germanium are practically equal. The smaller values for {311} and {100} of ~0.01 J/m^2 (i.e., $\sim1\%$) with respect to the {111} cases may be considered as the inaccuracy (more precisely, numerical uncertainties treating slabs with different orientations) of the used *ab initio* calculations.

The order of magnitude of the values measured for Si[17] (see Table I) agrees very well with the energies[28–30] calculated for the reconstructed surfaces. This also holds more or less for the energetical ordering $\gamma(111)<\gamma(311)<\gamma(100)<\gamma(110)$. Within the experimental results only the sequence of the {311} and {100} planes is interchanged. However, their energy difference is small in theory and experiment. The ordering obtained in other calculations[31,32] is the same. The other available experiment[16] found a surprisingly small an-

isotropy of the surface excess free energy per unit area with an unusual hierarchy $\gamma(100) < \gamma(311) < \gamma(110) \leq \gamma(111)$, which is not in agreement with the fact that cleavage happens for {111} surfaces. The anisotropy of the surface energies in Table I is remarkably increased for diamond, whereas it almost vanishes for germanium.

Table I also shows that the surface reconstruction and, hence, the actual surface geometry and preparation should play an important role for the shapes of crystallites or nanopyramids. The maximum change with respect to the energy of the surface with a bulk atomic arrangement amounts to 100% for the C(111) surface after a 2×1 reconstruction within the π-bonded chain model.[26] For Si(111) with the most favorable 7×7 reconstruction and Ge(111) with the $c(2\times8)$ reconstruction, the effect is much weaker.[28] Similar observations are made for the 2×1 (C) or $c(2\times4)$ (Si, Ge) reconstructions of a {100} surface.[26] The energy of Si and Ge(311) surfaces is substantially lowered by complicated 3×2 reconstructions involving reconstruction elements, such as adatoms, tetramers, and interstitials.[29] Indeed, there are experimental indications for reconstructed {311} surfaces on nanostructures. Pyramidal Si islands appearing at finite growth temperature on Si(001) substrates have {311} facets with a seemingly 3×1 reconstruction.[21] In the case of diamond(311), again a deviating behavior is found with a symmetric 2×1 tetramer reconstruction.[29] Such a 2×1 reconstruction has been observed for {311} facets of CVD diamond.[34,35] In the {110} cases the surface relaxation within a bond-contraction or a bond-rotation model[28] lowers the surface energy. Complicated long-range 16×2 reconstructions give only rise to a small additional energy gain (shown for Si), even considering adatom or adatom-tetramer-interstitial structural elements.[30] In Table I we present the lowest surface energy values found for 3×2 adatom-tetramer-interstitial and 2×1 adatom models for Si and Ge, respectively.[30]

C. Extrapolation

In order to investigate ⟨100⟩-oriented nanocrystals with pyramidal shape, one also needs the surface energies of {501} or {301} planes. Unfortunately, parameter-free calculations are not available for the absolute surface energies for the surfaces with those orientations. Such calculations[8,36] are restricted to the reconstruction geometries and the electronic structures. To estimate the $\gamma(501)$ and $\gamma(301)$ values we use the assumption that the surface free energy γ varies only weakly with the surface crystallographic orientation.

We formally consider a two-dimensional crystal in a plane perpendicular to the [010] direction with a vicinal surface plane, i.e., a surface plane that consists of a relatively high number of areas with [100] orientation being separated by steps of a certain height s_n (see Ref. 2). Such a surface has an orientation angle θ against the [100] direction. Each step is assumed to make a contribution δ to the total surface energy on the vicinal plane. With a step density $\tan\theta/s_n$, one can express the surface energy as

$$\gamma(\theta) = \gamma(100)\cos\theta + \frac{\delta}{s_n}\sin\theta. \tag{1}$$

The orientation vector [101] of the closest high-index surface (101) is found for $\theta=45°$. Assuming a continuous variation of the surface energy between the minima at [100] to [101],[16,17] one finds $\delta/s_n=\sqrt{2}\gamma(110)-\gamma(100)$. In the case of the $[n01]$ orientation $(n=5,3,1)$ it holds $\theta=11.31°, 18.43°, 45°$. Then expression (1) gives $\gamma(n01)=(1/\sqrt{n^2+1})[(n-1)\gamma(100)+\sqrt{2}\gamma(110)]$. One finds the energy values $\gamma(501)=6.12$ (C), 1.56 (Si), and 1.10 (Ge) J/m^2 and $\gamma(301)=6.26$ (C), 1.62 (Si), and 1.14 (Ge) J/m^2 using the values for reconstructed low-index surfaces from Table I.

III. EQUILIBRIUM CRYSTAL SHAPE

A. Wulff construction

The anisotropy of the surface free energy per unit area, $\gamma(hkl)$, with the orientation of a certain surface $\{hkl\}$ determines the equilibrium shape of small free crystals at a particular temperature T (here, small T compared to the melting temperature). The crystallite is assumed to be of at least mesoscopic or nanometer size so that edge and apex effects (more precisely, the corresponding energy terms) can be neglected (compared to the surface energy terms). Then, the equilibrium crystal shape (ECS) at constant (here, low) temperature T with fixed crystal(like) volume V and chemical potential μ of the group-IV material is determined by the minimum surface excess free energy F_s with respect to the total surface area $A=A(V)$ of the crystal,[3,26]

$$F_s = \oiint_{A(V)} \gamma(hkl)\,dA, \tag{2}$$

subject to the constraint of fixed volume V,

$$V = \int\int\int_{V(A)} dV. \tag{3}$$

The direction $\mathbf{n}$ of the area element dA is parallel to the facet normal $\langle hkl\rangle$. In the case of pure energetical studies of nanocrystals with pyramidal shape, one has to take into account additional constraints, such as the orientation and the shape of the basal plane of the pyramid. Formula (2) represents a bridge between microscopic and macroscopic approaches to the properties of matter. The surface free energies $\gamma(hkl)$ based on a full quantum-mechanical treatment of the motion of electrons are combined to calculate a thermodynamic potential, which is minimized with respect to the shape of a crystallite. The surface energies in Table I have been calculated under the assumption that the facets are large enough that their edges do not stabilize another reconstruction. Such a minimum distance of edges has been experimentally found for vicinal Si(111) surfaces. The 7×7 reconstruction with the large unit cell is still observable in STM for small terrace widths, at least up to 6 nm.[37]

The Wulff theorem based on the minimum surface excess free energy Eq. (2) and the constraint Eq. (3)[38–40] states that the ECS is not necessarily that of the minimum surface area of the free crystallite. It may be a complex polyhedron with the lowest total surface energy for a given volume. A minimal surface area occurs only for perfectly isotropic (i.e., con-

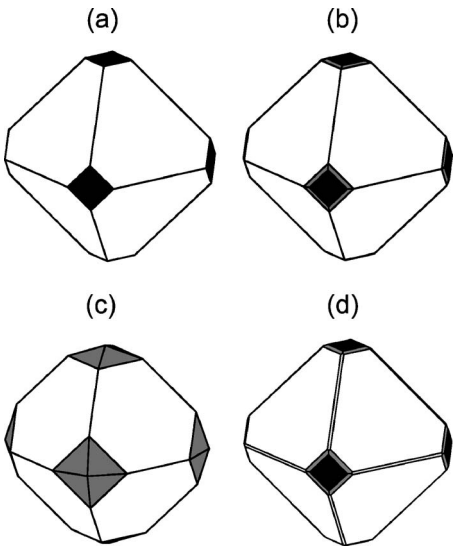

FIG. 1. Equilibrium shapes of diamond crystals based on the Wulff construction using basically γ values from Table I. In general, four surface orientations are considered, but in (a) only {111} and {100} facets. (b) Instead of the energy for the 2×1 reconstruction $\gamma(311)=5.11$ J/m^2, that for the 3×1 reconstruction $\gamma(311)=5.50$ J/m^2 is taken into account. (c) Values from Table I. (d) Values as for (b), but the energy of {110} facets is reduced to $\gamma(110)=4.91$ J/m^2. The areas with the orientation sequence $\langle100\rangle$, $\langle311\rangle$, $\langle110\rangle$, and {111} vary from black, dark gray, light gray, to white.

stant) values of $\gamma(hkl)$. The corresponding ECS is a sphere. The variation of γ with the normal $\mathbf{n}\|\langle hkl\rangle$ gives rise, on each surface element dA, to a force proportional to $\partial\gamma/\partial\mathbf{n}$ that tends to alter the direction at the same time as γ tends to shrink the area. Consequently, in general, the ECS cannot be a sphere.

B. Shape of diamond crystallites

Results of the Wulff construction of the ECS for diamond are plotted in Fig. 1. Essentially the surface energies calculated for the reconstructed low-index surfaces from Table I have been used. Taking into account only the surface with the lowest energy $\gamma(111)=4.06$ J/m^2, the cleavage face, one expects that the equilibrium geometry is a regular octahedron with eight {111} facets. However, already the inclusion of one further surface orientation, such as {100} [as shown in Fig. 1(a)], makes the octahedron irregular. The corners of the octahedron are truncated by {100} planes. A cubo-octahedron morphology appears with eight nonideal {111} hexagons and six {100}-oriented squares. Their areas depend on the surface energies, as long as $\sqrt{3}\gamma(111)<\gamma(100)$ (see Ref. 41). If $\gamma(111)$ is considerably less than $\gamma(100)$, then no truncation is expected. In the opposite limit, a constant ratio of the plane areas occurs.

Taking into account more surface planes with other orientations, the resulting shape depends very much on the absolute values of the surface energies. This is also clearly demonstrated in Fig. 1. Using the energy $\gamma(311)=5.50$ J/m^2 for the symmetric 3×1 adatom-dimer reconstruction[29] instead of the lower value given in Table I [Fig. 1(b)], the cubo-octahedral shape of the nanocrystallites is basically conserved; but the {100} squares are surrounded by stripes corresponding to {311} facets. Diamond particles with exactly such a morphology have been observed after deposition by microwave-plasma CVD (see Ref. 24). Decreasing the surface energy of the {311} facets to the value $\gamma(311)=5.11$ J/m^2 (Table I) for the 2×1 reconstruction, the corner truncation does not happen anymore, and no {100} facets occur [see Fig. 1(c)]. Instead, the octahedron corners are rounded by small square-based pyramids with four {311} facets. This prediction of the ECS for diamond clearly shows the importance of (113) surface orientation for diamond for possible future applications.

Another example for the strong influence of the γ values is shown in Fig. 1(d). The values constructing Fig. 1(b) have been used, but the surface energy of the {110} planes is remarkably reduced to $\gamma(110)=4.91$ J/m^2. In contrast to Fig. 1(b), the sharp edges between {111} facets disappear and {110} planes form stripes along the former edges. Such a shape with {111}, {100}, {311}, and {110} facets has been observed for high-pressure–high-temperature synthetic diamonds.[23] Their surfaces have major growth sectors of {111} and {100} type and some minor sectors of {311} and {110} type.

We state general agreement with morphologies observed for grown diamond crystallites. Not only {111} are facets present, in particular, {311} facets dominate in the corners of the ECS as shown in Fig. 1(c). However, there is perhaps no direct relationship between absolute surface energies of reconstructed clean surfaces and crystallography, which the above description suggests. The real surfaces may be contaminated by adsorbed species or influenced by defects. Adsorbates and defects may change the surface reconstruction and, hence, the corresponding surface energy. In addition, the observed crystallite shapes may tend to be dominated by the growth process of the crystal rather than the energetics itself. One fact is related to the orientation dependence of the growth rate. For instance, there are indications that the CVD growth rate on {100} surfaces is faster than that of the {111} side-growth rate.[42] The preferential growth along a $\langle100\rangle$ direction clearly influences the resulting morphology of a crystallite.

C. Shape of Si and Ge crystallites

Figure 2 shows results of the Wulff construction of the ECS for silicon and germanium. In Figs. 2(b) and 2(c) we used calculated parameters of the surface energies $\gamma(hkl)$ for the reconstructed {111}, {110}, {100}, and {311} surfaces of silicon and germanium given in Table I. For the purpose of comparison, the ECS for Si is presented in Fig. 2(a) for measured surface energies.[17] According to energies given in Table I, Fig. 2(a) shows that the most stable surfaces have $\langle111\rangle$ orientation with the next lowest ones being {100}, {311}, and {110} surfaces with similar energies. Large {111} facets and smaller {100} facets occur on the surface of a crystallite. Between these facets, smaller {311} and {110} facets are observable. No sharp edges between a {111} and a {100} facet or between two {111} facets appear. According to

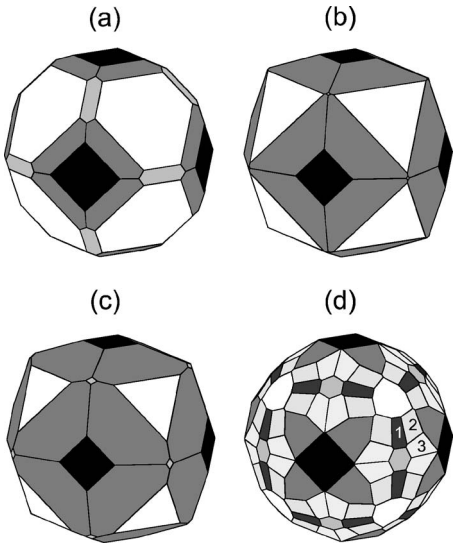

FIG. 2. Equilibrium shapes of Si (a,b) and Ge (c,d) crystals based on the Wulff construction using (a) experimental values, (b,c) calculated values, or (d) equal values γ for many surface orientations in the stereographic triangle (see Ref. 44). In (a)–(c), four surface orientations are considered. The areas with the orientation sequence ⟨100⟩, ⟨311⟩, ⟨110⟩, and {111} vary from black to white. In (d) more high-index surfaces are taken into consideration. The notations 1, 2, and 3 represent {331}, {21 9 29}, and {15 3 23} facets, respectively.

the experimental γ values, the equilibrium shape is thus, to a good approximation, a tetrakaidecahedron.[17] Taking the calculated γ values into account, the {110} facets almost vanish as a consequence of the large $\gamma(110)$ value as shown by their small contributions in the corners between four {311} facets in Fig. 2(b). In addition the areas of the {311} facets are increased because of the low value of $\gamma(311)$.

One of the results of the ECS construction is the possible stability evaluation of a surface with a certain orientation. We have checked a possible occurrence of the Si(411) surface on the ECS. A Si(411)2×1 reconstruction has been observed experimentally. The value of its surface energy calculated within an *ab initio* method lies between those for (111)2×1 and (100)2×1 surfaces.[43] Consequently, it has been concluded that Si(114) is a stable planar surface.[43] To be consistent within the computational method used here, we assume γ of Si(411)2×1 to be equal to 1.44 J/m^2 as found for the lowest left buckled π-bonded chain Si(411)2×1 reconstruction from our calculations.[28] Surprisingly, despite a such low γ the {411} facets do not occur on the ECS, indicating that a (411) surface is not stable in the equilibrium in contrast to the (100) or (311) ones. However, narrow stripes would appear between the {100} and {311} facets if an additional reduction of $\sim$0.015 J/m^2 is assumed, which also indicates that the absence of {411} facets might be related to the inaccuracy of our approximations. The sensitivity of the ECS with respect to the absolute values of the surface energies again shows that modifications of the facet geometry, e.g., due to reconstruction, may drastically change the surface morphology of a crystal.

The last tendency is enforced for germanium as demonstrated in Fig. 2(c). Since the energies for the surface orientations ⟨111⟩, ⟨311⟩, and ⟨100⟩ are nearly the same, large {111}, {311} and {100} facets are visible. However, {311} facets give the largest area. Only small diamond-shaped {110} planes occur between {311} facets (note, larger than in the the case of Si). Nearly equal energies of the most stable surface orientations give a probability that several other high-index orientations have a similar γ and are therefore stable in the Ge case. To check this we include possible candidates with equal γ. In addition to the above-mentioned four surface orientations, we also study the high-index surfaces {313}, {15 3 23}, and {21 9 29}, which have been reported to be stable and, hence, do not facet into other stable surfaces.[44] The resulting ECS is represented in Fig. 2(d). All considered surface orientations appear on it. In general, a Ge crystal tries to reach a "sphere" shape. The largest facets are the {111}, {311}, and {100}, whereas the {110} facets occur with a smaller area. Each of the sets of high-index {15 3 23} or {21 9 29} surfaces contributes to the 48 facets. The corresponding values of the total area per family are close to that for {311} facets that take the largest area.

IV. SHAPE OF PYRAMIDAL CRYSTALLITES

A. Total energy and surface energy

The shape of a large, isolated, three-dimensional island grown on a certain substrate is determined by its total energy[1,45]

$$E_{\text{total}} = E_{\text{elastic}} + E_{\text{surface}} + E_{\text{edge}}. \tag{4}$$

For coherently strained or partially relaxed islands, the leading terms are the elastic relaxation energy E_{elastic} and the surface energy E_{surface} of the strained object connected with a substrate. E_{elastic} is the gain in deformation energy when the material forms a strained island instead of a biaxially strained film. E_{surface} is the cost in surface energy due to the creation of facets on the sides of the island corrected by the fact that the island base forms an interface to the substrate or the corresponding wetting layer. E_{edge} is the energy cost for the creation of sharp edges. Because of the interplay of local strain distribution and shape, the scaling behavior of E_{elastic} with the volume V may also include nonlinear terms in addition to the main linear term. E_{surface} and E_{edge} scale with the volume as $V^{2/3}$ and $V^{1/3}$, respectively. For an isolated island to form at all in preference to a film with the same volume, E_{total} must be negative.

Still, it is questionable if such a model (4) based partially on the macroscopic continuum theory may really apply to nanometer-sized systems. Nevertheless, here we go a step further in the simplifications and discuss trends essentially restricting to the surface energy based on Table I. Usually, E_{edge} is estimated to be negligible, provided the island size is not too small. In the case of III–V compounds this fact has been shown for nanometer-sized quantum dots.[45] The characteristic length scale for small dots is about 5–10 nm. The renormalization of the surface free energies per unit area γ is also more or less negligible because of surface stress.

Changes up to 11% leave the prediction for the equilibrium shape qualitatively unchanged.[45] The elastic energy E_{elastic} is very important for the absolute value of the total energy of an island. However, for a given qualitative island shape its variation with the geometry parameters is also small, for InAs islands on GaAs(001) $<10\%$.[46] For large islands that are not dislocation-free, the energy contribution E_{elastic} should be mainly determined by the elastic energy of a fictitious two-dimensional film with the same volume. As a consequence, in the following we qualitatively discuss the pyramidal shape of islands only on the basis of the surface energies. We are still using the request of a minimum surface energy F_s [Eq. (2)]. In addition to the constraint of a fixed volume V [Eq. (3)], we also consider two other constraints, the orientation of the pyramid and the shape of the pyramid base plane. That means, the only considered influence of the substrate used in the epitaxial growth is the normal of the base (parallel to the surface normal of the substrate) and its shape. The nanopyramids are assumed to be large enough, so that the γ values for reconstructed surfaces in Table I can be applied. The relationship of the pyramidal geometry and the surface energy is discussed in Sec. IV B.

B. Deformation of pyramids

During epitaxial growth and ripening, the shape of the islands may change.[47] One example is the truncation of the small pyramids, which results in a reduced aspect ratio (i.e., their height h divided by a characteristic base length a). For any regular pyramid, the truncation is described by a parameter $(0<\varepsilon<1)$

$$\varepsilon = 1 - \frac{\gamma_{\text{top}}}{\gamma_{\text{side}}} \cos\theta, \tag{5}$$

where θ is the angle between negative orientation of the base (or the orientation of the truncating plane) and one of the side facets. Thereby, we have assumed that the surface energy of the pyramid base is zero as a rough approximation for the surface energy between pyramid and substrate or wetting layer. The deviation $(1-\varepsilon)$ of the parameter ε [Eq. (5)] from the case of an untruncated pyramid $\varepsilon=0$ dominates the aspect ratio $h/a=m(1-\varepsilon)\tan\theta$, where the geometry parameter m is equal to $1/2\sqrt{3}$ and $1/2$ for triangle- and square-based pyramids, respectively. For a pyramid with volume V the minimum surface energy F_s is given by

$$F_s = \frac{s\gamma_{\text{side}}}{\cos\theta}\left(\frac{3}{sm\tan\theta}V\right)^{2/3}(1-\varepsilon^3)^{1/3}, \tag{6}$$

where the geometry parameter s is $\sqrt{3}/4$ for the triangle base and 1 for the square base. The comparison of the total surface energies for a given volume V gives an indication for the favored orientations of the facets and the trend for truncation of the pyramid.

Growth of Ge on Si(111) surfaces leads to nucleation of three-dimensional islands, which consist of {113} facets as sidewalls and a flat top (111) facet.[48] The model of such a pyramidal island is presented in Fig. 3 with a $(\bar{1}\bar{1}\bar{1})$ triangle base, a (111) top, and three equivalent (113), (131), and (311)

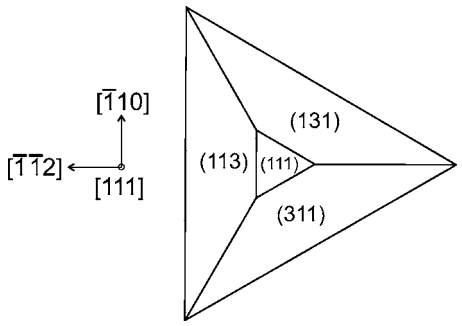

FIG. 3. Top view of frustum of a [111]-oriented pyramid with {311} facets.

facets. In this case the angle θ is given by $\arccos(5/\sqrt{33})$, i.e., 29.5°. During the epitaxial growth, the aspect ratio of an island may change as a function of the coverage. However, the form of the island is always a frustum of a tetrahedron, and the complete pyramid with {113} facets is never reached.[48] Using values from Table I, one therefore finds for the parameter $\varepsilon=0.31$ (C), 0.15 (Si), and 0.11 (Ge). The truncation can be interpreted as a consequence of the ECSs presented in Figs. 1 and 2. They show the appearance of large {111} facets for diamond and relatively small {111} facets for Ge. A reduction of the surface energies of (111) faces until values corresponding to a 2×1 reconstruction [i.e., 1.45 (Ge) and 1.05(Si) J/m^2 (Ref. 28)] also fulfills the condition for the truncation. For Ge the aspect ratio h/a results to 0.145 [with $\gamma(111)$ corresponding to $c(2\times8)$] or 0.15 [with $\gamma(111)$ corresponding to 2×1]. Values for grown pyramids vary from 0.1 to 0.135.[48] Consequently, taking into account only surface energies, there is a tendency for truncation of a [111]-oriented triangle-based pyramid shown in Fig. 3.

At low growth temperatures or low Ge coverages the small Ge islands grown on Si(100) substrates are rectangular-based huts or square-based pyramids with {501} (Refs. 11–14) or sometimes {301} (Ref. 8) facets. In the case of InAs quantum dots on GaAs(100) substrates, {101} facets have also been studied.[1,46,49] In order to model the pure surface energetics of small islands of this type, we consider a $(00\bar{1})$ square base with a $[00\bar{1}]$ normal and four equivalent facets with $[01n]$, $[0\bar{1}n]$, $[10n]$, and $[\bar{1}0n]$ orientations ($n=1,3,5$) [see Fig. 4(a)]. The tilt angle θ of the facets is given by $\arccos(n/\sqrt{1+n^2})$, i.e., 45°, 18.43°, or 11.31°. The truncation of the considered pyramids takes place for all group-IV elements. However, the tendency to cut a pyramid is stronger for the smaller n. For germanium the parameter, Eq. (5), amounts to $\varepsilon=0.37(n=1)$, $0.21(n=3)$, and $0.11(n=5)$. Similar dependencies are found for Si and C. Assuming the value $\gamma(001)=1.05$ J/m^2 for Ge, which corresponds to a 2×1 reconstruction, the value of truncation amounts only to $\varepsilon=0.06$ and the aspect ratio is $h/a=0.006$. Experimentally, the latter quantity was observed equal to 0.1 what nearly corresponds to the complete pyramid.

At higher Ge coverages of Si(100) substrates, large Ge islands, so-called domes, appear. The domes are more rounded and display a multifaceted surface.[14] They are

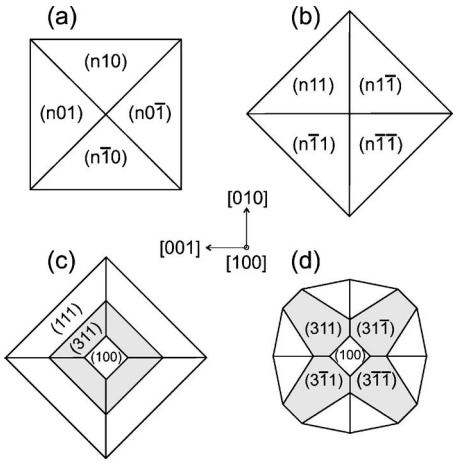

FIG. 4. Top view of [100]-oriented pyramids or domes with $\{n01\}$ ($n=5,3,1$), $\{n11\}$ ($n=3,1$), and $\{100\}$ facets. In (d) the facets without denotation represent $\{15\ 3\ 23\}$ facets.

bounded by $\{113\}$ and $\{15\ 3\ 23\}$ facets. In the intermediate coverage regime, the occurrence of $\{105\}$ is also discussed. Here, we neglect the rounding and only study another type of square-based pyramids with $[001]$ orientation and four equivalent facets with $[11n]$, $[1\bar{1}n]$, $[\bar{1}1n]$, and $[\bar{1}\bar{1}n]$ surface normals, where usually $n=3$ but also other values, such as $n=1$ may be considered [see Fig. 4(b)]. Such shapes have been suggested for Si nanocrystallites.[20] In their case, the tilt angle θ of the facets $\arccos(n/\sqrt{n^2+2})$, i.e., $54.74°(n=1)$, $25.24°(n=3)$, and $6.21°(n=13)$, depends dramatically on the growth time. For short growth times, even $\{1\ 1\ 13\}$ facets with $n=13$ have been observed. They change over into $\{111\}$ facets with $n=1$ for longer growth time.

Within the simplified picture [Eq. (6)] of the restriction to surface energies, one finds that $\{n11\}$ facets are more favorable than $\{n01\}$ facets. For large Ge nanocrystals, this finding is in agreement with the observation of $\{311\}$ facets instead of surfaces with $\langle 501\rangle$ orientations.[14] According to Eq. (6), the total surface energy is three times smaller in the case of $\{311\}$ facets.

Again, we have to state that the total energy reduction may be also a driving force for the truncation of the pyramids with $\langle n11\rangle$ facet orientations. The largest parameters ε occur for $n=1$. Using the values from Table I one has $\varepsilon=0.19$ (C), 0.42 (Si and Ge). Consequently, the tendency for truncation is most pronounced for silicon and germanium. For $n=3$, the values of ε with 0.09 (Si) and 0.08 (Ge) are much smaller. Truncation will not happen for $n>1$ in the diamond case. For Si islands, it has been observed that pyramids with $\{111\}$ facets transform into ones with $\langle 311\rangle$ orientation at elevated temperature. Allowing that both $\{113\}$ and $\{111\}$ facets appear on the sidewalls, the ratio of their heights $h(311)/h(111)$ is given by $2\gamma(001)/[\sqrt{11}\gamma(311)-\sqrt{3}\gamma(111)]-1$. According to Table I, this results in 0.23 (0.30) for Si (Ge) or 0.32 (0.37) if the energy of the (111) surface is reduced to the value for the 2×1 reconstruction.

For Si and Ge, the main difference between the ECSs derived by Wulff constructions shown in Fig. 2 and pyramid shapes discussed in this section (i.e., models of experimentally observed crystallites) is the number of occurring steep facets. In particular, for [100]-oriented pyramids one may consider another shell of $\{311\}$ facets. This would give eight additional $\{311\}$ facets, but they do not appear on islands during epitaxial growth. The reason seems to be related to a very large angle θ of these facets with the $\langle 100\rangle$ orientation, namely, 72.45°. Other facets corresponding to orientations with smaller θ are more likely. Surfaces with $\langle 111\rangle$ and $\langle 110\rangle$ orientations with θ equal to 54.74° and 45°, respectively, are good candidates. It is interesting that $\{110\}$ facets, which almost disappear on the ECS [see Figs. 2(b) and 2(c)], could lead to large facets on the [100]-oriented pyramid in addition to the discussed four $\{113\}$ facets. For Si and Ge, in this case four facets with $\langle 110\rangle$ orientation will occur near the bottom of the pyramid and a rounding of the base will take place [cf. Figs. 4(a) and 4(b)]. Moreover, for Si pyramids $\{111\}$ facets have indeed been observed. That is not the case for heteroepitaxially grown Ge islands, for which also $\{110\}$ facets have not been detected. Experimentally observed $\{15\ 3\ 23\}$ facets have only a tilt angle of $\theta=33.63°$. A model of such a pyramid is shown in Fig. 4(d). Taking into account only surface energies, the probability for facets with this surface orientation to appear in the corner between two neighboring $\{311\}$ facets is rather high. It happens if the relation $\gamma(15\ 3\ 23)\lesssim 1.7\gamma(311)$ is fulfilled as the condition for the minimum of the total surface energy. As mentioned above for Ge (the softest material under consideration), surface energies of different orientations do not vary so much. Therefore, other effects than the energetics, e.g., strain, should stabilize such lower sloped high-index facets.

For the surface energies given in Table I with a not-too-strong variation with the surface orientation, we conclude that deviations from the ideal shape of the pyramids, such as truncation or rounding, are favorable within considerations restricted to the pure energetics of the facets. However, these results can only indicate a trend. Taking into account the strain of the pyramids, the volume dependence of the total energy (4) is changed from $E_{\text{total}}=\alpha V^{2/3}$ to $E_{\text{total}}=\alpha V^{2/3}-\beta V$ (see Ref. 50). Optimizations of energy functionals of such a type may give modified results. In particular, it is expected that the effects of truncation and rounding depend on the pyramid volume. Consequently, shape transitions as the transition from pyramids to domes observed for Ge on Si(100) can be only described taking into account the strain energy and/or kinetics effects and not only using an equilibrium theory with a restriction to the total surface energy.

V. SUMMARY

We presented results for absolute surface energies of group-IV materials for various orientations that have been obtained by *ab initio* slab calculations for reconstructed surfaces. Apart from diamond, for which the $\{111\}$ cleavage faces are really energetically favored, the energy variation for surfaces with orientations $\langle 111\rangle$, $\langle 311\rangle$, and $\langle 100\rangle$ is rather weak for Si and Ge. Only the value for $\{110\}$ facets is substantially larger.

The absolute surface energies are used to discuss the equilibrium shapes of small three-dimensional crystals and [111]- and [100]-oriented pyramids or domes. We showed that the equilibrium crystal shapes depend very much on the absolute values of the surface energies. As a consequence we observed a shape variation from diamond via silicon to germanium. Interestingly, we predicted that {311} facets should occur on the ECS of diamond. In the case of Ge, a more spherical shape has been predicted. Neglecting the influence of edge bonding and strain, we generally observed tendencies for [111]- and [100]-oriented pyramids to be deformed, i.e., tendencies toward truncation, base deformation, or faceting. The strength of such a trend depends on the geometry and the absolute values of the surface energies.

ACKNOWLEDGMENTS

We thank Jürgen Furthmüller for helpful discussions. We also acknowledge financial support from the Deutsche Forschungsgemeinschaft (Project No. Be1346/16-1) and the European Community in the framework of the Research and Training Network NANOQUANTA (Contract No. NMP4-CT-2004-500198).

[1] V. A. Shchukin and D. Bimberg, Rev. Mod. Phys. **71**, 1125 (1999).
[2] H. Lüth, *Solid Surface, Interfaces and Thin Films* (Springer-Verlag, Berlin, 2001).
[3] J. A. Venables, *Introduction to Surface and Thin Film Processes* (Cambridge University Press, England, 2000).
[4] J. Tersoff and F. K. LeGoues, Phys. Rev. Lett. **72**, 3570 (1994).
[5] M. Zinke-Allmang, L. C. Feldman, and M. H. Grabow, Surf. Sci. Rep. **16**, 377 (1992), and references therein.
[6] I. Daruka, J. Tersoff, and A.-L. Barabási, Phys. Rev. Lett. **82**, 2753 (1999).
[7] K. O. Ng and D. Vanderbilt, Phys. Rev. B **52**, 2177 (1995).
[8] P. Raiteri, D. B. Migas, L. Miglio, A. Rastelli, and H. von Känel, Phys. Rev. Lett. **88**, 256103 (2002).
[9] I. N. Stranski and V. L. Krastanov, Akad. Wiss. Lit. Mainz Abh. Math. Naturwiss. Kl. **146**, 797 (1939).
[10] D. J. Eaglesham and M. Cerullo, Phys. Rev. Lett. **64**, 1943 (1990).
[11] Y.-W. Mo, D. E. Savage, B. S. Swartzentruber, and M. G. Lagally, Phys. Rev. Lett. **65**, 1020 (1990).
[12] A. Vailionis, B. Cho, G. Glass, P. Desjardins, D. G. Cahill, and J. E. Greene, Phys. Rev. Lett. **85**, 3672 (2000).
[13] G. Medeiros-Ribeiro, A. M. Bratkovski, T. L. Kamins, D. A. A. Ohlberg, and R. S. Williams, Science **279**, 353 (1998).
[14] F. M. Ross, R. M. Tromp, and M. C. Reuter, Science **286**, 1931 (1999).
[15] A. Malachias, S. Kycia, G. Medeiros-Ribeiro, R. Magalhães-Paniago, T. I. Kamins, and R. S. Williams, Phys. Rev. Lett. **91**, 176101 (2003).
[16] J. R. Bermond, J. J. Métois, X. Egéa, and F. Floret, Surf. Sci. **330**, 48 (1995).
[17] D. J. Eaglesham, A. E. White, L. C. Feldman, N. Moriya, and D. C. Jacobson, Phys. Rev. Lett. **70**, 1643 (1993).
[18] H. Hirayama, M. Hiroi, and T. Ide, Phys. Rev. B **48**, 17331 (1993).
[19] L. Vescan, K. Grimm, and C. Dieker, J. Vac. Sci. Technol. B **16**, 1549 (1998).
[20] M. Shibata, Y. Nitta, K. Fujita, and M. Ichikawa, Phys. Rev. B **61**, 7499 (2000).
[21] V. Shklyaev and V. Zielasek, Surf. Sci. **541**, 234 (2003).
[22] H. Baumgärtner, F. Kaesen, H. Gossner, and I. Eisele, Appl. Surf. Sci. **130–132**, 747 (1998).
[23] G. Kowalski, M. Moore, G. Gledhill, and Z. Maričić, Diamond Relat. Mater. **5**, 1254 (1996).
[24] K. W. Chae and Y.-J. Baik, Diamond Relat. Mater. **8**, 1261 (1999).
[25] S. T. Lee, H. Y. Peng, X. T. Zhou, N. Wang, C. S. Lee, I. Bello, and Y. Lifshitz, Science **287**, 104 (2000).
[26] F. Bechstedt, *Principles of Surface Physics* (Springer-Verlag, Berlin, 2003).
[27] J. J. Métois and P. Müller, Surf. Sci. **548**, 13 (2004).
[28] A. A. Stekolnikov, J. Furthmüller, and F. Bechstedt, Phys. Rev. B **65**, 115318 (2002).
[29] A. A. Stekolnikov, J. Furthmüller, and F. Bechstedt, Phys. Rev. B **67**, 195332 (2003); **68**, 205306 (2003).
[30] A. A. Stekolnikov, J. Furthmüller, and F. Bechstedt, Phys. Rev. B **70**, 045305 (2004); Phys. Rev. Lett. **93**, 136104 (2004).
[31] J. H. Wilson, J. D. Todd, and A. P. Sutton, J. Phys.: Condens. Matter **2**, 10259 (1990); **3**, 1971(E) (1991).
[32] G. H. Gilmer and A. F. Bakker, Mater. Res. Soc. Symp. Proc. **209**, 135 (1991).
[33] R. J. Jaccodine, J. Electrochem. Soc. **110**, 524 (1963).
[34] G. Janssen, J. J. Schermer, W. J. P. van Enckevort, and L. J. Gilling, J. Cryst. Growth **125**, 42 (1992).
[35] K. A. Snail, Z. P. Lu, R. Weimer, J. Heberlein, E. Pfender, and L. M. Hanssen, J. Cryst. Growth **137**, 676 (1994).
[36] Y. Fujikawa, K. Akiyama, T. Nagao, T. Sakurai, M. G. Lagally, T. Hashimoto, Y. Morikawa, and K. Terakura, Phys. Rev. Lett. **88**, 176101 (2002).
[37] http://uw.physics.wisc.edu/~himpsel/wires.html
[38] G. Wulff, Z. Kristallogr. Mineral. **34**, 449 (1901).
[39] C. Herring, Phys. Rev. **82**, 87 (1951).
[40] C. Herring, *The Use of Classical Macroscopic Concepts in the Surface-Energy Problem*, in: *Structure and Properties of Solid Surfaces*, edited by R. Gomer and C. S. Smith (University of Chicago Press, Chicago, 1953), p. 5.
[41] W. A. Harrison, *Electronic Structure and the Properties of Solids* (Dover, New York, 1989).
[42] C.-S. Yan, Y. K. Vohra, H.-K. Mao, and R. J. Hemley, Proc. Natl. Acad. Sci. U.S.A. **99**, 12523 (2002).
[43] S. C. Erwin, A. A. Baski, and L. J. Whitman, Phys. Rev. Lett. **77**, 687 (1996).
[44] Z. Gai, W. S. Yang, R. G. Zhao, and T. Sakurai, Phys. Rev. B **59**, 15230 (1999).

[45] Q. K. K. Liu, N. Moll, M. Scheffler, and E. Pehlke, Phys. Rev. B **60**, 17008 (1999).
[46] N. Moll, Ph.D. thesis, Technical University Berlin, 1998.
[47] K. C. Lin, Y. H. Chiu, J. H. Lin, and W. W. Pai, Nanotechnology **16**, S63 (2005).
[48] B. Voigtländer, Surf. Sci. Rep. **43**, 127 (2001).
[49] L. G. Wang, P. Kratzer, N. Moll, and M. Scheffler, Phys. Rev. B **62**, 1897 (2000).
[50] F. M. Ross, J. Tersoff, and R. M. Tromp, Phys. Rev. Lett. **80**, 984 (1998).